

Pulsar electrons detection in AMS-02 experiment. Model status and discovery potential.

Jonathan Pochon*

Instituto de Astrofísica de Canarias, C. Vía Láctea, 38200, La Laguna, Tenerife, Spain

November 20, 2018

Abstract

The measurements of electrons (e^\pm) from cosmic rays have begun a new era a few years ago with high precision experiments like PAMELA [1] and Fermi-LAT [2]. The positron fraction seems to indicate an unknown component above the standard background described in the last 40 years, mostly by HEAT [3]. In the last few years, the PAMELA satellite has confirmed the positron fraction excess above 10 GeV, and studying Fermi-LAT data, the electron flux seems to be steeper than expected. While these new measurements have not closed the debate, results from AMS-02 [4] are expected to reach the accuracy needed to determine a full description of this excess and possibly give some evidence on the possible source. We will present in this note, the AMS-02 capacity in the case of positrons produced by pulsars.

Introduction

The context of the positron-electron cosmic rays can be summarized by a series of measurements in disagreement with what we understand. Indeed, since the 70s most of the experiments, namely TS93 [5], HEAT [6] [7], Caprice [8], AMS-01 [9], PAMELA [10], exhibit a deviation from the standard framework in the positron fraction ($\frac{e^+}{e^+ + e^-}$), represented by figure 1 (left). Looking at the total flux of e^\pm , observations by Fermi-LAT [11], balloon experiments like ATIC [12] and ground ones like HESS [13] present a steeper behavior summarized in figure 1 (right). The standard propagation model can well explain the cosmic rays energy spectrum above 1 GeV, shown in studies by Moskalenko and Strong [14]. However, the positron fraction above 10 GeV remains unexplained. All models from propagation to source candidates were improved trying to reproduce observational data. During propagation, most of the models are consistent between them, the data uncertainty allowing high degeneracy models [15], in particular for the measurement of the nuclei ratio B/C , Be^9/Be^{10} . Regarding source candidates, two approaches seem to be preferred. The first one, is to consider the closest astrophysical objects able to produce positron-electron pairs, like e.g. pulsars [16] [17]. Some pulsars are sufficiently close and energetic to be responsible of positrons deviation. The second possibility, is to consider dark matter particles, which can produce e^\pm through annihilation [18] [19] or decaying [20]. So far, only PAMELA and ATIC have claimed or confirmed such a deviation from standard background. For PAMELA (figure 1 left) the positron fraction above 10 GeV is growing, while for ATIC, the electron flux forms a "bump" around 400 GeV (figure 1 right). However, the Fermi-LAT measurements do not agree with the ATIC bump result, establishing only a mildly harder e^\pm flux [21]. In this context, AMS-02 will be a powerful detector able to give crucial informations on positrons that are directly connected to this possible extra contribution with respect to

*email: jgpochon@iac.es

expected background. This note will discuss the topic of electrons produced by pulsars, and will present the AMS-02 capacity.

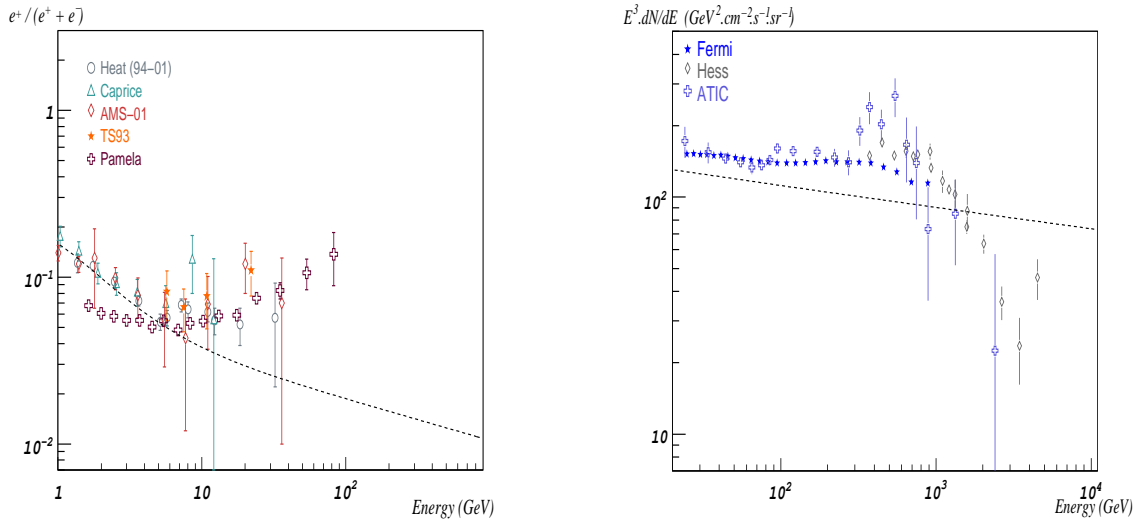


Figure 1: *Left: Positron fraction for TS93 [5], HEAT [6] [7], Caprice [8], AMS-01 [9] and PAMELA [10] compared with expected background [14]. Right: Electrons flux for Fermi-LAT, HESS and ATIC compared to the standard background.*

1 Electrons coming from pulsars

Since the discovery of pulsars in 1967 [22], most of the models agree with measurements like periodicity, but some unknowns still remain, e.g. the gamma-ray production. Electron production in the pulsar has not yet been observed, and their detection would be an interesting discovery. Through systematic surveys, pulsars are well studied and basic characteristic are available. Figure 2 (left) shows that for the Australia Telescope National Facility (ATNF) [23], observed pulsars in the Galaxy cover a good range in distance.

1.1 Pulsar e^\pm production

Gamma-ray production in pulsars, giving electron-positron pairs, can be modeled by two mechanisms of relativistic particle acceleration: the *polar cap* (PC) [24] [25] and the *outer gap* (OG) [26]. EGRET [27] [28] has shown evidence, for several pulsars, of a pulsed gamma-ray emission at GeV scale, giving confidence to the fact that the magnetosphere must be involved for the charged particle acceleration. P. Goldreich and W.H. Julian [29] have demonstrated that magnetic field tears away electrons from the pulsar surface. The distribution of charged particles in the magnetosphere screens the electric field $E_{||}$ parallel to the magnetic field ($\mathbf{B} \cdot \mathbf{E} = 0$), allowing the co-rotation of the whole system. But in some locations, the condition $\mathbf{B} \cdot \mathbf{E} = 0$ is not maintained and particle can be accelerated following field lines. From there, a volume named *light cylinder* can be defined as a cylinder with the rotation axis as symmetry axis, and with radius equal to the co-rotating part. Outside this frontier, magnetic field lines are not closed. The acceleration can take place mostly in two locations. The first one is close to the surface near the magnetic pole, a situation described by the *polar cap* model (PC). The other, located between the last closed magnetic field line and the surface along the null electric surface defined by the condition $\mathbf{\Omega} \cdot \mathbf{B} = 0$, where $\mathbf{\Omega}$ is the pulsar rotational velocity, a configuration dubbed the *outer gap* model (OG). Briefly, in both of them, quasi-static electric field accelerates the relativistic electrons, producing electron-positron pairs. The PC model consists of two steps. First one inside the acceleration region,

a charged particle (e^\pm) is taken away from the surface due to the electric field radiating gamma-ray by synchrotron. Then these gamma-rays create an e^\pm pair, through magnetic field or by interaction with thermal X-rays from the pulsar surface. These secondaries are moving toward the light cylinder and then can escape. On the other hand, the OG model proposes a pair production from photon-photon interaction. e^\pm follow field lines radiating gamma-rays which interact with low energy photons (X-rays, infrared) producing e^\pm pairs, and then able to escape outside the light cylinder. First difference between the two models is that the OG location is farther than the PC one, so more distant from the magnetic field giving harder flux, while the PC configuration has a bigger contribution at low energy. Chi et al. [30] estimate that these two models give comparable total energy output in e^\pm . A criterion for the OG existence is given by Zhang et al. [31] and implies that g , ratio between dimension of the OG and radius of the light-cylinder, should be less than one. The OG existence condition can be expressed as [31]

$$g = 5.5P^{26/51}B_{12}^{-4/7} < 1. \quad (1)$$

with P being the pulsar period in s and B_{12} the pulsar magnetic field in 10^{12} G. Conventionally, pulsars with the condition $g < 1$ are gamma-ray pulsars. The ATNF [23] compiled the most complete and updated pulsar catalogue[32], comprising 1794 pulsars, with 272 being of the "gamma-ray" type. Figure 2 (left) demonstrates that "gamma-ray" pulsars in that catalogue cover a good range of distances in the Galaxy, and of ages.

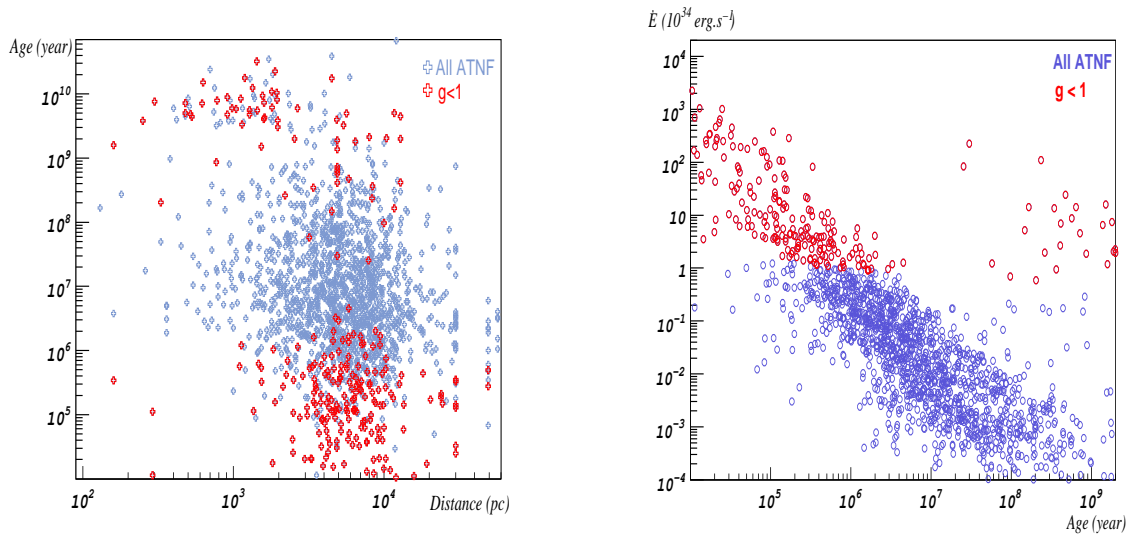


Figure 2: *Distribution of pulsars from the ATNF catalogue [23] including "gamma-ray" ones ($g < 1$). Left: Pulsar age versus distance. Right: Pulsar spin-down power versus age.*

1.2 Characteristics of the pulsar electron emission

The measurement accuracy on rotation frequency ($\Omega = 2\pi/P$ [Hz]) and frequency derivative give an estimation on the pulsar age. A pulsar can be modeled like a rotating neutron star with a dipolar magnetic field misaligned with its rotation axis, producing pulsed radiation from the magnetic poles. In this way, the electromagnetic energy comes from rotational energy following a braking law of $\dot{\Omega} \propto -\Omega^3$, implying an energy variation $\dot{E} = I\Omega\dot{\Omega}$, proportional to the moment of inertia I . The pulsar rotational velocity can be written as [33]

$$\Omega(t) = \frac{\Omega_0}{(1 + t/\tau_0)^{1/2}} \quad (2)$$

where Ω_0 is the initial spin frequency and τ_0 a decay time expressed as

$$\tau_0 = \frac{3c^3 I}{B^2 R_s^6 \Omega_0^2} \quad (3)$$

where I is the moment of inertia of the pulsar. $\tau_0 \sim 10^4$ years for nominal parameters [34]. \dot{E} is compared to the pulsar age in figure 2 (right), which establishes that the oldest objects have the lowest \dot{E} . At the same time, for each age sample, "gamma-ray" ones have the higher \dot{E} . Mature pulsars could contribute to e^\pm flux because produced particles are no longer trapped [30]. This framework allows us to derivate an estimated total released energy from a pulsar. Indeed, the upper limit to the rate of energy for electron-positron pairs is given by

$$\dot{E} = I\Omega\dot{\Omega} = \frac{1}{2}I\Omega_0^2 \frac{1}{\tau_0} \frac{1}{(1 + \frac{t}{\tau_0})^2} \quad (4)$$

From this equation, assuming an efficiency factor f_{e^\pm} for e^\pm pair production, the total energy that a mature pulsar ($t \gg \tau_0$) has injected in magnetic dipole radiation is [36] [37]

$$E_{tot} \approx \frac{f_{e^\pm}}{2} I\Omega_0^2 \approx f_{e^\pm} \dot{E} \frac{T^2}{\tau_0} \quad (5)$$

where T is the typical age and \dot{E} the spin-down power. The expected value for the efficiency factor is $f_{e^\pm} \sim \text{few } \%$ [36]. Other models, like Harding and Ramaty [38], Chi, Cheng and Young [39], and Zhang and Cheng [40], provide another E_{out} expression. As a consequence of energy losses from the source to the earth, the maximum energy of electrons reaching the observer is expressed as $E_{max} = 3.10^3/t_5 \text{ GeV}$, with t_5 representing the electron age in 10^5 years unit. This implies that after 10^5 years, the maximum electron energy will be 3 TeV . E_{max} indicates the maximum reach by the pulsar electron spectrum. As a direct consequence, the oldest the pulsar, the lowest is the E_{max} . Figure 3 (left) illustrates, for the whole ATNF catalogue, that $E_{out}^{e^\pm}$ decreases with E_{max} , and that most of "gamma-ray" pulsars have a spectrum component above 10-100 GeV. Figure 3 (right) indicates that only three of the "gamma-ray" pulsars inside 1 kpc radius are able to contribute above 100 GeV.

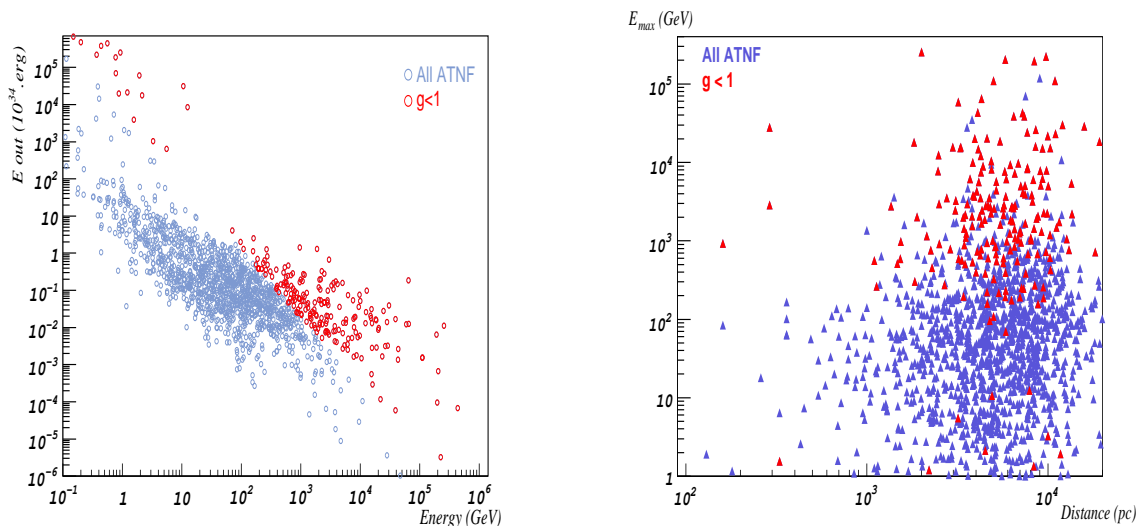


Figure 3: *Left: Standard pulsar $E_{out}^{e^\pm}$ versus E_{max} reached. Right: E_{max} reached by pulsar versus pulsar distance.*

The spectral shape is limited at the energy range by E_{max} but also because e^\pm cannot be accelerated to arbitrarily high energies and a cut-off is expected around the TeV scale. Below that, we will assume a power law $Q(E_e) \propto E^{-\alpha}$. EGRET [27] [28] observations of galactic pulsars give a power index α for gamma-ray spectra between 1.4 and 2.2. Assuming

the power law measurement of cosmic electrons(positrons) of around 3.1 (3.3) [41], a pulsar contribution with enough intensity is expected to appear in the electron spectrum. Table 1 summarizes some properties for a sample of pulsars and supernova remnant Loop I [37] [42] which will be represented like a pulsar. All of the objects being close enough and with a large spin-down energy loss, giving total energy released E_{tot}^{out} . In order to contribute above 10 GeV, these pulsars must be close-by (~ 100 - 1000 pc) and their age must be less than $3 \cdot 10^7$ years. Geminga and Monogem are the two most probable and/or popular sources for the positron fraction excess. The two are experimentally interesting because of the intensity and the spectrum range.

Table 1: *Data for selected nearby pulsars.*

Name	Dist. (pc)	Age (years)	g	E_{tot}^{out} (10^{50} GeV)	E_{max} (GeV)
Geminga [J0633+1746]	160.	$3.42 \cdot 10^5$	0.70	74.	930.
Monogem [B0656+14]	290.	$1.11 \cdot 10^5$	0.14	9.	2850.
Vela [B0833-45]	290.	$1.13 \cdot 10^4$	0.70	17.	28040.
B0355+54	1100.	$5.64 \cdot 10^5$	0.61	281.	562.
Loop I [SNR]	170.	$2 \cdot 10^5$	-	43.	1584.

From this short-list, one can understand the importance of the energy range for the detector. Since pulsars can contribute from GeV to TeV scale, it is crucial to see a cut-off and/or decrease to validate the pulsar contribution. For example, PAMELA seems to be too low in energy to detect such cut-off, while AMS-02 and Fermi-LAT with their extended range up to TeV may detect it.

2 Flux at Earth after propagation

2.1 Solution of diffusion equation

After production of e^\pm , these particles mostly lose energy by synchrotron radiation (SR) and inverse Compton scattering (ICS). Their motion depends on the galactic magnetic field, which enables the direction reconstruction for charged particles. These processes are calculated by solving the transport equation in the standard diffusion approximation (neglecting convection), which for local sources can be expressed with a spherical symmetry, and reduced to the form [43]

$$\frac{\partial}{\partial t} \frac{dn_e}{dE_e} = \frac{K(E_e)}{r^2} \frac{\partial}{\partial r} \left[r^2 \frac{\partial}{\partial r} \frac{dn_e}{dE_e} \right] + \frac{\partial}{\partial E_e} \left[b(E_e) \frac{dn_e}{dE_e} \right] + Q(E_e) \quad (6)$$

Here, dn_e/dE_e is the number density of e^\pm per unit energy, $K(E_e)$ is the diffusion parameter, $b(E_e)$ is the rate of energy loss, and $Q(E_e)$ the source term. We assume $K(E_e) \equiv K_0(E_e/1\text{GeV})^\gamma$, with K_0 and γ specified in table 2, where scenario MAX maximizes the positron flux and MIN minimizes it, and $b(E_e) = -bE_e^2$ with $b = 10^{-16}\text{GeV}^{-1}\text{s}^{-1}$.

Table 2: *Different scenarios for diffusion parameters [44].*

Scenario	K_0	γ
MAX	$1.8 \cdot 10^{27}$	0.55
MED	$3.4 \cdot 10^{27}$	0.7
MIN	$2.3 \cdot 10^{28}$	0.46

Assuming a power law injection, the solution of equation 6 is given by [43]

$$\frac{dn_e}{dE_e} = \frac{Q(E_e)}{\pi^{3/2}r^3}(1 - btE_e)^{\alpha-2} \left(\frac{r}{r_{diff}}\right)^3 e^{(r/r_{diff})^2} \quad (7)$$

where $E < E_{max} \approx 1/(bt)$, and by $dn_e/dE_e = 0$ otherwise, with r_{diff} being

$$r_{diff} \approx 2\sqrt{K(E_e)t\frac{1 - (1 - E/E_{max})^{1-\gamma}}{(1 - \gamma)E/E_{max}}} \quad (8)$$

The local e^\pm flux from pulsars is fixed by pulsar distance r , the time of injection t which can be the pulsar age $t = T$ for mature pulsars, and the normalization of the injected flux. In this way, the local flux is just $J(E_e) = c(dn_e/dE_e)/(4\pi)$. Figure 4 establishes energy spectra for different injection times t and two different diffusion scenarios (see tab. 2). From these figures, one can see that contributions from old pulsars can be negligible compared to young ones; at the same time, for young sources, the diffusion time limits the contribution. Moreover, one understands that propagation parameters are key for spectrum shape and intensity. Indeed, in the MED scenario (see tab. 2), contribution from low energy is relatively more important than for the MAX scenario, while the shape of the MAX energy spectra is more easily distinguishable than in the MED case. From the experimental detection point of view and in particular for AMS-02, it is clear that the MAX scenario is preferred because of the flux shape. In any case, having a strong cut-off at E_{max} could be a way to identify each pulsar contribution. The next sub-section will present the contribution in positron fraction of a sample of close-by pulsars.

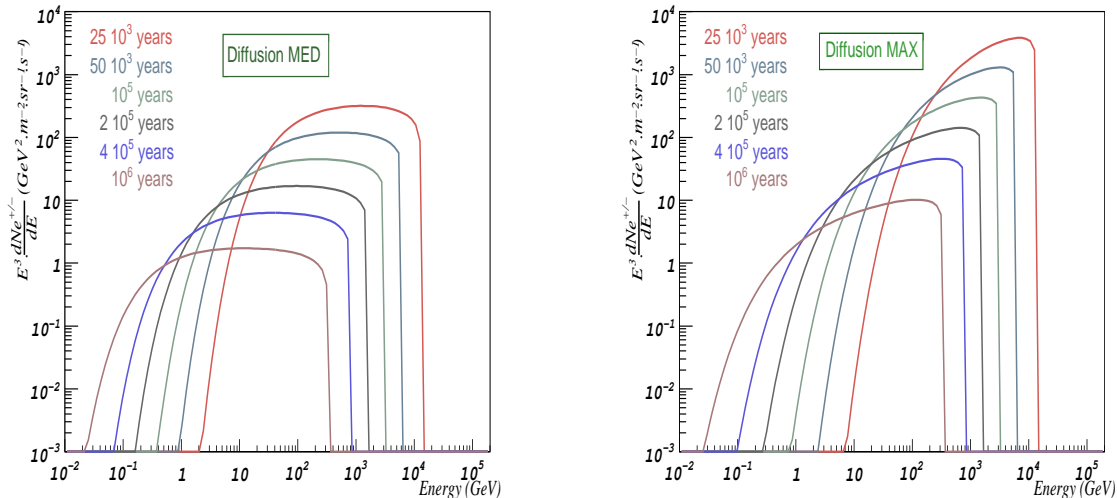


Figure 4: Energy spectra of electrons at different injection time from a source at $r = 160$ pc, $\alpha = 2$, and $E_{out} = 6 \cdot 10^{50}$ GeV for two diffusion scenarios: MED (left) and MAX (right) (see tab. 2).

2.2 Positron fraction from nearby pulsars

As first experimental study, only the closest pulsars, described in table 3, will be assumed as sufficient sources to explain the positron excess. Electrons flux will be determined for each one using equation 7 with $\alpha = 2$. Positron fraction is adjusted with these sources for typical propagation parameters set: MAX, MED and MIN presented in table 2. Results are shown in table 1 where each pair production efficiency f_{e^\pm} pulsar are adjusted to reproduce PAMELA positron fraction for all propagation scenarios. As expected, the scenario which maximizes electrons are performed with the lowest f_{e^\pm} . In this case, some % for f_{e^\pm} are sufficient to explain positron fraction which is in agreement with expectations [36]. The other

extremum case, MIN scenario, needs almost 30% of the total energy released by the pulsar, which seems unlikely. Values for f_{e^\pm} are chosen arbitrary keeping some proportionality between propagation case, except for B0355+54 pulsar which have a strong f_{e^\pm} to create an irregularity in the total contribution.

Table 3: *Data for selected nearby pulsars. Pair production efficiency f_{e^\pm} are calculated for different propagation scenario (see table 2).*

Name	E_{tot}^{out} (10^{50} GeV)	f_{e^\pm}		
		(MAX)	(MED)	(MIN)
Geminga [J0633+1746]	74.	0.04	0.15	0.33
Monogem [B0656+14]	9.	0.03	0.10	0.25
Vela [B0833-45]	17.	0.03	0.10	0.25
B0355+54	281.	0.30	0.30	0.40
Loop I [SNR]	43.	0.04	0.10	0.33

Figures 5 illustrate positron fraction prediction for AMS-02 for the extreme cases MAX scenario (left) and MIN scenario (right) using electrons and positrons background adjusted by Baltz et al. [45]. For these predictions, AMS-02 acceptance is taken to be $\mathcal{A}_{e^\pm} = 0.045 m^2 \cdot sr$. Further informations on the AMS-02 electron/proton separation and its acceptance can be found in the literature [46] [47]. Two remarks can be made about AMS-02 electron acceptance. Firstly, below 10 GeV, the acceptance is lower than this mean value but the rate of cosmic rays is strong enough, so electron flux will still be high and will compensate the acceptance. Secondly, at energy above 500 GeV, the electron/proton separation will be more challenging for the detector, while at the same time the proton contamination is decreasing with energy, which could help to keep a good separation. For these reasons, the electron acceptance will be assume energy-independent. For the MAX scenario 5 (left), a structure from pulsars contribution can be detected by AMS-02 and a clear decreasing appears above 500 GeV.

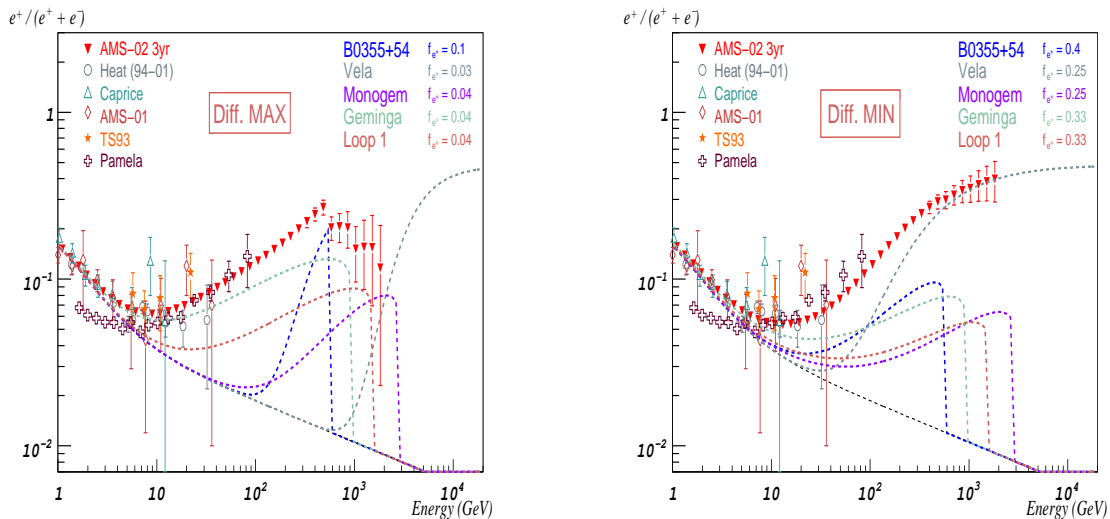


Figure 5: *Positron fraction reproduced by pulsar contributions ($\alpha = 2$) for two propagation scenarios with AMS-02 capacity: MAX (left) and MIN (right) (see table 3).*

The MIN scenario, figure 5 (right), presents a total contribution without irregularity increasing above TeV scale. This scenario give a smooth contribution and it would be

difficult to distinguish single pulsar contribution, even in the case of multiple f_{e^\pm} values. The same problem comes with the MED scenario which gives also a continuous flux from pulsars. To conclude, propagation scenario MAX case gives the best experimental conditions with pair production parameters f_{e^\pm} as expected by models up to a few percent. In this scenario, pulsars with a large f_{e^\pm} (B0355+54 in our case) must appear like a peak in the spectrum or giving a clear cut-off detectable by AMS-02, like seen in figure 5 (left). On the other hand, the MIN scenario may smooth all contributions making almost impossible the pulsar distinction, and it implies important f_{e^\pm} , around 30 %, to reproduce PAMELA data (figure 5 (right)), indicating that pulsars couldn't be the unique contribution to this excess. For this study, electrons background was assumed for a mean value, Delahaye et al. [35] presented uncertainties for leptons background where background can be higher and, in this case pulsars flux may be lower.

2.3 Positrons flux from pulsars continuum

In section 2.2, only nearby pulsars had been considered sufficient to reproduce positron fraction. ATNF catalogue gives 184 more "gamma-ray" type pulsars above 1 kpc, and an age compatible with a contribution above 10 GeV. To determine a contribution for all these pulsars, the same f_{e^\pm} is assumed. Pulsars continuum is calculated with $f_{e^\pm} = 0.03$ in figure 6 (left) for the MAX scenario. The total contribution have similar electrons production to Geminga pulsar, in the same condition. A simple way to represent the whole faraway pulsars could be to use a pulsar-like adjustment assuming a cut-off above hundreds GeV. In this section, a cut-off around 2 TeV will be assumed like extremum case where pulsars continuum can contribute at high energies. According the distance, pulsars continuum may contribute mostly above 50 GeV. Others studies [36] [40] based on random distribution in the galaxy for a giving pulsar birthrate give contribution at lower energies because they are considering all pulsars even old ones, which are out this study. Indeed, we consider pulsars able to participate at the positrons excess at high energy.

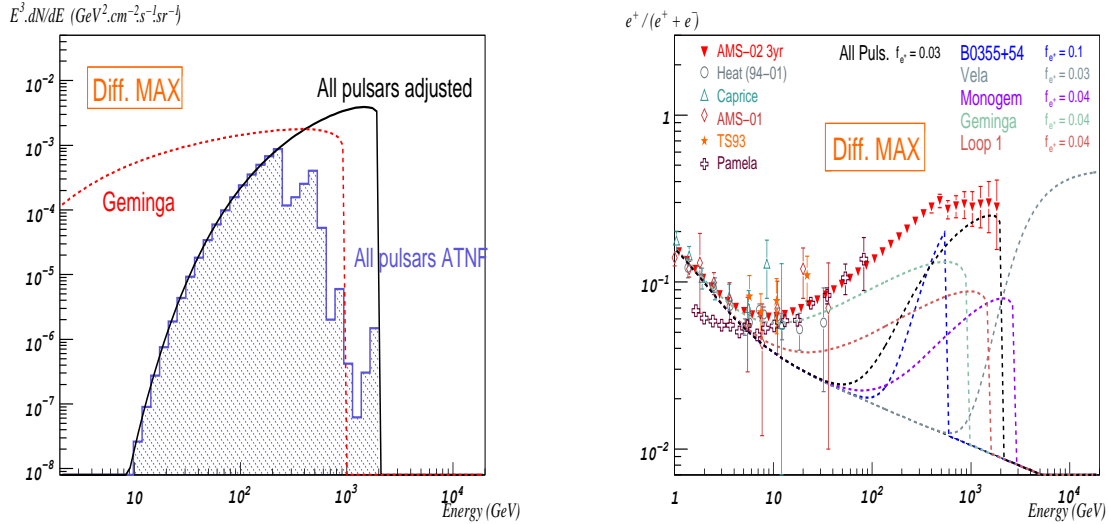


Figure 6: Left: Electrons flux from all ATNF gamma-ray pulsars ($r > 1$ kpc) compared to Geminga with $f_{e^\pm} = 0.03$. Right: Positron fraction reproduced by nearby pulsars and pulsars continuum with AMS-02 capacity.

Pulsars adjustment from figure 6 (left) is used in same conditions with nearby pulsars to reproduce PAMELA positron fraction in figure 6 (right). Positrons from faraway pulsars should diminish structure effects and cut-off in the positron fraction. Above 500 GeV, continuum should hide individual pulsar giving plateau-like with a low decreasing rate. In the best case, choosing a lower cut-off for the continuum, in between 700 GeV to 1 TeV,

will give a similar shape with a decreasing a bit bigger without cut-off. Assuming same conditions for all pulsars, continuum should participate to positron fraction at high energy diminishing detector capacity to determine primary sources. In the continuum case, AMS-02 should observe at least a plateau above 500 GeV with a slow decreasing.

3 Anisotropy: strong evidence for pulsar contribution?

The propagation of positrons-electrons does not allow to pinpoint each possible e^\pm source, reducing the chance of constraining models, for example, which sources are responsible for the excess from dark matter. One possibility proposed by Mao & Shen [48] is that the closest pulsars can induce an anisotropy in the pulsars direction. Although propagation affects electron trajectory, close-by pulsars can induce a small dipole anisotropy, which should be present at sufficiently high energy [48]. Anisotropy will be discussed for electrons-positrons and positrons case.

3.1 Anisotropy in the e^+e^- flux

In a very general way, the anisotropy of the e^\pm flux associated with diffusive propagation can be calculated as [49]

$$\delta = \frac{I_{max} - I_{min}}{I_{max} + I_{min}} = \frac{3K|\nabla(dN_e/dE_e)|}{c(dN_e/dE_e)} \quad (9)$$

where $\nabla(dN_e/dE_e)$ is the gradient of e^\pm density. In the case of energy-independent diffusion anisotropy, Mao & Shen [48] proposed an estimation of the maximum expected anisotropy as

$$\delta_{max} = \frac{3}{2c} \frac{r}{t} \quad (10)$$

where r and t are respectively the distance and age of the pulsar. This simple relation forces us to choose not only the closest pulsars, but also young ones. Table 4 shows some expected energy-independent pulsar anisotropies. Vela being a young pulsar gives a strong anisotropy with respect to Geminga or Monogem.

Table 4: *Maximum anisotropy for selected nearby pulsars.*

Name	Dist. (pc)	Age (years)	δ_{max} (%)
Geminga [J0633+1746]	160.	$3.42 \cdot 10^5$	0.23
Monogem [B0656+14]	290.	$1.11 \cdot 10^5$	1.28
Vela [B0833-45]	290.	$1.13 \cdot 10^4$	12.5
B0355+54	1100.	$5.64 \cdot 10^5$	0.95
Loop I [SNR]	170.	$5.64 \cdot 10^5$	0.15

For energy-dependent diffusion, inserting Eq. 7 in 9, anisotropy can be expressed as

$$\delta = \frac{3}{2c} \frac{r}{t} \frac{(1-\gamma)E/E_{max}}{1 - (E/E_{max})^{1-\gamma}} \frac{N_e^{Puls}}{N_e^{tot}} \quad (11)$$

where N_e^{Puls} and N_e^{tot} are e^\pm contribution from pulsars and from the electron background, taken from [41]. From the detection point of view, to observe an anisotropy at the 2σ level, the observations must satisfy the condition $\delta \geq 2\sqrt{2}/\sqrt{N_{evts}}$ where N_{evts} is the number of events collected above an energy threshold.

Figures 7 show anisotropies expected for the two closest pulsars: Geminga and Monogem, where each pulsars flux is determined like in section 2.2. In the figure 7 (left), Geminga and Monogem are set like in the table 3 to adjust PAMELA positron fraction with others

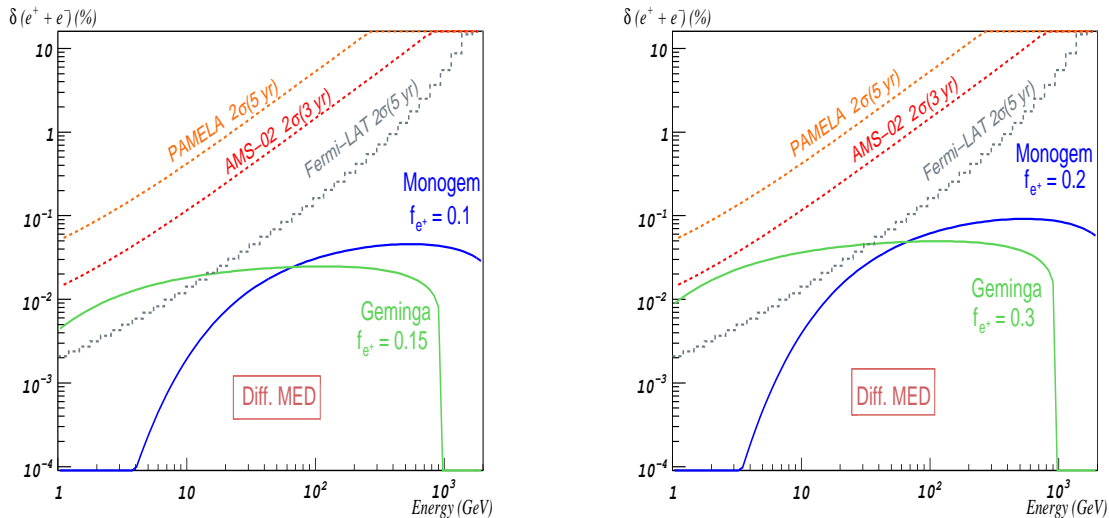


Figure 7: Anisotropy in e^\pm flux for Geminga and Monogem pulsars with sensitivity expected for AMS-02, PAMELA and Fermi-LAT experiments for MED propagation scenario (see table 3). Geminga and Monogem are set to reproduce alone positron excess (right), or with others pulsars (left) (see section 2.2).

close pulsars, and figure 7 (left) presents a new configuration where Geminga and Monogem only contribute to positron excess with higher individual e^\pm production. These anisotropies are represented for MED propagation scenario, and compared to the sensitivity expected of the experiments PAMELA, Fermi-LAT and AMS-02 with standard background. The main difference between experiments sensitivity is explained mostly by their electron acceptance: Fermi-LAT have $\mathcal{A}_{Fer}^{e^\pm} \sim 1.5 - 2 \text{ m}^2 \cdot \text{sr}$ [11], for AMS-02 it is $\mathcal{A}_{AMS}^{e^\pm} \sim 0.045 \text{ m}^2 \cdot \text{sr}$ [46], and for PAMELA, $\mathcal{A}_{PAM}^{e^\pm} \sim 0.002 \text{ m}^2 \cdot \text{sr}$ [1]. After five years, PAMELA will reach $\delta > 0.5\%$ at 2σ above 10 GeV remaining too high to detect such anisotropy. AMS-02 and even more Fermi-LAT may be able to distinguish an anisotropy. For AMS-02 within three years, sensitivity should be the same order than Geminga anisotropy for the case where Geminga and Monogem have sufficient e^\pm production to reproduce PAMELA data as it appears in figure 7 (left). To prevent the misunderstanding of anisotropy results, it would be better to look for anisotropy above 10 GeV where starts the positron excess, for this reason looking for e^\pm anisotropy, Fermi-LAT should be the best experiment with $\delta > 0.015\%$ at 2σ above 10 GeV. Indeed in figure 7 (left), Fermi-LAT with five years statistic can establish an anisotropy for Geminga from low energy to 10 GeV in the multiple pulsars hypothesis. For the strong pulsars case, presented by 7 (right), Fermi-LAT should extend the accessible energy range for Geminga until 30 GeV, and may almost reach Monogem anisotropy. This study shows how it will be difficult for experiments to deal with anisotropy having sensitivity and anisotropy values very close. Besides the influence on the f_{e^\pm} , propagation will play a role in the spectrum pulsar shape and therefore should modify in the pulsar anisotropy. For the MAX scenario, contributions at low energy will diminish where most of the statistic are expected, and for the MIN one pulsars will give flat distribution and some anisotropy for Fermi-LAT below 10 GeV. For the e^\pm anisotropy, Fermi-LAT must be the best experiment to provide some anisotropy informations.

3.2 Anisotropy in e^+ flux: powerful detection

Electrons-positrons anisotropy is interesting because of high statistic reachable by Fermi-LAT experiment. An another possibility is to consider only positrons flux. Indeed, studying positron is a direct way to connect to the primary e^\pm source. Therefore, anisotropy in e^+ flux is the best way to characterize a close-by source and to constrain it, this study was

well presented by Busching et al. [50]. Fermi-LAT can not perform this measurement, because is not able to distinguish positrons from electrons. PAMELA and AMS-02 have both magnets to determine sign particle. The average field inside the PAMELA magnet is $0.4 T$ [1], AMS-02 with its superconductor magnet having a bending power of $0.86 T \cdot m^2$ [51], will differentiate between electrons and positrons above 300 GeV.

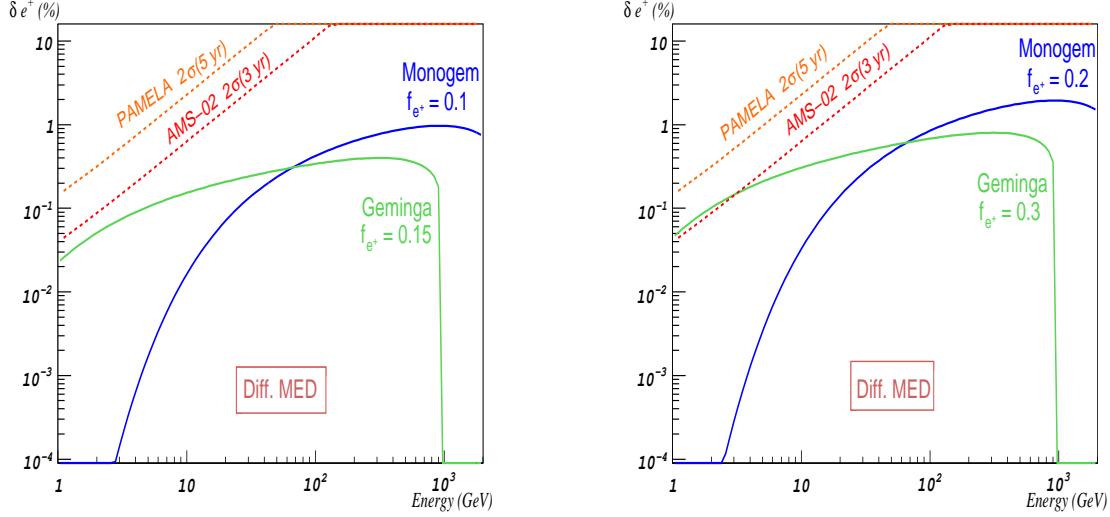


Figure 8: Anisotropy in e^+ flux for Geminga and Monogem pulsars with sensitivity expected for AMS-02 and PAMELA experiments for MED propagation scenario (see table 3). Geminga and Monogem are set to reproduce alone positron excess (right), or with others pulsars (left) (see section 2.2).

The study performed with e^\pm , in section 3, is now applied to e^+ . Figures 8 present e^+ anisotropy for MED propagation with sensitivity at 2σ level for PAMELA after 5 years and AMS-02 after 3 years. PAMELA will get $\delta > 0.1\%$ above 1 GeV after 5 years where δ must be around 0.01% to see e^+ anisotropy. Figure 8 (left) confirms AMS-02 needs close pulsars with most of the energy transferred to e^\pm to have sufficient discovery capacity like shown in figure 8 (right). AMS-02 is in best condition than in the previous section (3), AMS-02 will be able to reach pulsar anisotropy below 10 GeV if few pulsars like Monogem and Geminga produce most of the e^\pm excess. The difficulty for AMS-02 is to perform an anisotropy analysis below 10 GeV.

3.3 Discussion on anisotropy detection

In previous sections, Geminga and Monogem were supposed to be sufficiently distant from each other to induce an individual dipole. Nevertheless, according particles propagation and respective pulsar galactic coordinates, $Monogem(b, l) = (201.11^0, +08.25^0)$ and $Geminga(b, l) = (195.13^0, +04.27^0)$, one can assume that total measured anisotropy could be sum of the two. Indeed, propagation could be helpful for anisotropy detection by merging Geminga and Monogem electrons. Taking MED propagation set, sum of the two pulsars anisotropy, in figure 9 (left), gives a too weak anisotropy increasing to be considered like an enhancement.

An another hypothesis which can be discussed is the pulsar background. Faraway pulsars (section 2.3) can be added to the standard electron-positron background N_e^{tot} in the equation 11. Looking at pulsars continuum, propagation must be sufficiently diffuse to produce an isotropic contribution overlapping Monogem and Geminga contributions. This new anisotropy is estimated for Geminga and Monogem in figure 9 (right) with continued lines, compared to the case without pulsars background in dashed line. The biggest effect is expected at high energy where anisotropy would be lower and unreachable with detector sensitivity. Therefore, pulsar background should not affect anisotropy measurement. An

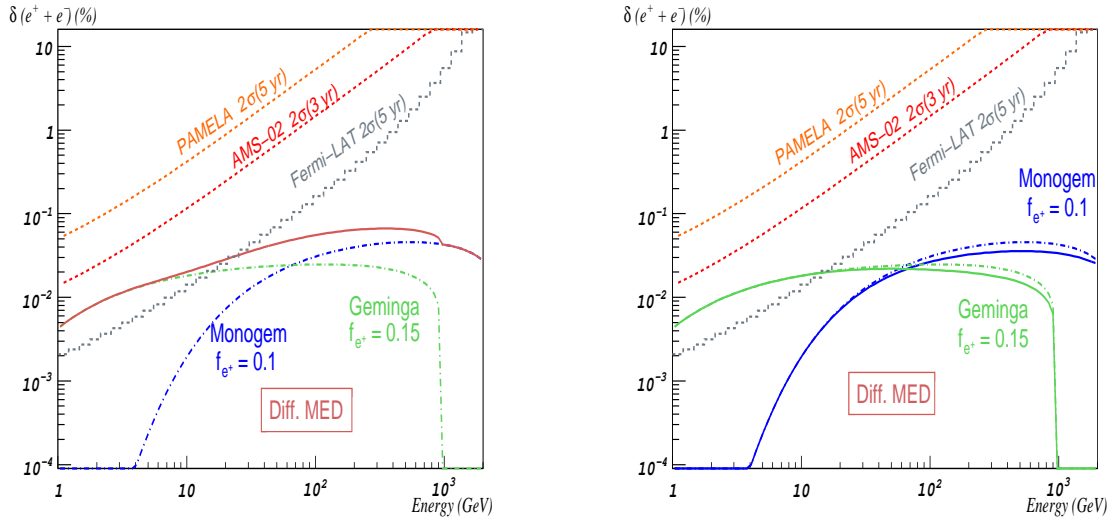


Figure 9: *Left: Anisotropy in e^\pm flux for sum of Geminga and Monogem contributions for MED diffusion. Right: Geminga and Monogem with pulsars background (continued line) and without (dashed line) for MED diffusion with sensitivity expected for PAMELA, AMS-02 and Fermi-LAT.*

other aspect must be discussed about anisotropy, which is its own standard fluctuation. Indeed, geomagnetic field must produce some effects in anisotropy map inducing some natural anisotropy which must be understood before any anisotropy claim.

Conclusion

For almost four years, positron fraction is studied with new generation experiment, PAMELA had confirmed the increase of positrons above 10 GeV which can indicate a primary e^+ source like pulsars, and Fermi-LAT has observed electrons flux with great accuracy and it seems to be above standard background. Next years, AMS-02 will provide a positron fraction at higher energy with better accuracy than PAMELA, and Fermi-LAT will extend his energy range from GeV to TeV. In this article, we considered that positron excess is the result of electron-positron pairs production in nearby pulsars, affected by different propagation scenarios. AMS-02 will be the only experiment able to investigate positrons at high energy, and therefore constraint more efficiently e^+ sources. The closest pulsars can contribute to positron fraction and propagation should modify contributions, in two extremes ways: propagation scenario which maximizes electrons flux (MAX) should allow each pulsar to be noticed, and the other hand the one minimizing (MIN) the flux will smooth all contributions giving a continuum flux. The MAX scenario is preferred from experimental point of view, and it is in agreement with pulsars models implying low pair production parameters, around %. In this configuration, AMS-02 will be the only experiment able to confirm pulsars implication. The others propagation parameters sets will not allow to distinguish each pulsar, and for the one minimizing positron flux (MIN), pulsars should not be able to produce the whole positron contribution. Without direct detection of pulsars, anisotropy studies in the positron and positron-electron flux will be powerful test to establish pulsar production. Geminga and Monogem should induce enough e^\pm anisotropy to be detected in five years with 2σ significance by Fermi-LAT, and AMS-02 will be able to detect an e^+ anisotropy at the same level after 3 years if Geminga and Monogem are the only contribution to positron excess. Others candidates, like supernova remnant (SNR) or Dark Matter, can participate to leptons flux, and AMS-02 will be a helpful detector studying from leptons to nuclei constraining each contributions.

References

- [1] PAMELA experiment <http://pamela.roma2.infn.it>
- [2] Fermi-LAT experiment <http://www-glast.stanford.edu>
- [3] S. Barwick et al. *Nucl. Inst. & Med.*, 400 (1997) 34
- [4] AMS-02 experiment <http://ams.cern.ch>; <http://ams.nasa.gov>
- [5] Golden et al. *ApJ*, 457 (1996), L103
- [6] Ma Duvernois et al. *ApJ*, 559 (2001), 296-303
- [7] S. Barwick et al. *Phys. Rev. Lett.*, 75 (1995) 390; *ApJ*, 482 (1997) L191
- [8] Boezio et al. *ApJ*, 532 (2000), 653
- [9] Alcaraz et al. *Phys. Lett. B*484 (2000) 10
- [10] O. Adriani et al. *Nature* 458, (2009) 607-609
- [11] A.A. Abdo et al. *Phys. Rev. Lett.* 102 (2009) 181101
- [12] J. Chang et al. *Nature* 456, (2008) 362-365
- [13] H.E.S.S collaboration *Phys. Rev. Lett.* 101 (2008) 261104
- [14] I.V. Moskalenko and A.W. Strong *ApJ*, 493 (1998a) 694
- [15] D. Maurin et al. *arXiv:astro-ph/0212111*
- [16] J.H. Taylor and D.R. Stinebring *ARA&A* 24 (1986) 285
- [17] D.C. Backer *Pulsars (Galactic and Extragalactic Radio Astronomy, 1988)* pp. 480-521
- [18] M. Cirelli and A. Strumia *arXiv:0808.3867* (2008)
- [19] L. Bergstrom et al. *arXiv:0808.3725* (2008)
- [20] J. Zhang et al. *arXiv:0812.0522* (2008)
- [21] D. Grasso et al. *arXiv:0905.0636* (2009)
- [22] A. Hewish et al. *Nature* 217 (1968) 709
- [23] ATNF catalogue <http://www.atnf.csiro.au/research/pulsar/psrcat/>
- [24] M.A. Rudermans and P.G. Sutherland *ApJ*, 196 (1975) 51
- [25] J. Arons *ApJ*, 266 (1983) 215A
- [26] K. Cheng et al. *ApJ*, 300 (1986) 522C; *ApJ*, 300 (1986) 500C;
- [27] D.J. Thompson et al. *ApJ*, 436 (1994) 229
- [28] J.M Fierro et al. *ApJ*, 447 (1995) 807
- [29] P. Goldreich and W.H. Julian *ApJ*, 157 (1969) 869
- [30] X. Chi et al. *ApJ*, 459 (1996) L83
- [31] L. Zhang & K.S. Cheng *ApJ*, 487 (1997) 370
- [32] R.N. Manchester et al. *ApJ*, 129 (2005) 1993
- [33] M.S Longair "High Energy Astrophysics", Vol II, Cambridge University Press, 2nd edition (1994)
- [34] F.A. Aharonian et al. *A&A* 294,(1995) L41-L44
- [35] T. Delahaye et al. *A&A*.501,(2009) 821-833
- [36] D. Hooper et al. *JCAP* 0901 (2009) 025.
- [37] Stefano Profumo *arXiv:0812.4457*
- [38] J.K. Daugherty and A.K. Harding *ApJ*, 252 (1982) 337
- [39] X. Chi et al. *ApJ*, 459 (1996) L83
- [40] L. Zhang & K.S. Cheng *A&A*, 368 (2001) 1063
- [41] Barwick et al. *ApJ*, 498 (1998) 779

- [42] **T. Kobayashi et al.** *ApJ*, 601 (2004) 340, *arXiv:astro-ph/0308470v1*
- [43] **A.M. Atoyan et al.** *Phys. Rev.*, D52 (1995) num. 6
- [44] **T. Delahaye et al.** *Phys. Rev.*, D77 (2008) 063527, *arXiv:0712.2312*
- [45] **E.A. Baltz and J. Edsjo** *Phys. Rev.*, D59 (1999) 023511.
- [46] **J. Pochon** *PhD. thesis (2005): <http://tel.archives-ouvertes.fr/tel-00010164/fr>*
- [47] **P. Maestro** *PhD. thesis (2003): <http://ams.cern.ch/AMS/Reports/AMSnotes2003>*
- [48] **C.Y. Mao et C.S. Shen** *Chinese Journal Phys.* vol. 10 no. 1 (1972)
- [49] **P. Ginzburg & S.I. Syrovatskii** *The Origin of Cosmic Rays (1964) N.Y. Macmillan*
- [50] **I. Bsching et al.** *ApJ*, 678 (2008) L39, 0804.0220
- [51] **AMS-02 Collaboration** *Nucl. Instrum. Meth.* A588 (2008) 227-234